PACS: 71.28.+d, 75.10.Lp, 75.40.Cx

G.E. Grechnev[1], A.S. Panfilov[1], I.V. Svechkarev[2], A. Czopnik[2], D. Kaczorowski[2], A. Hackemer[2], O. Eriksson[3]

PRESSURE EFFECT ON MAGNETIC PROPERTIES OF UX_3 COMPOUNDS

[1]B. Verkin Institute for Low Temperature Physics and Engineering
of the National Academy of Sciences of Ukraine
47 Lenin Ave., Kharkov, 61103, Ukraine

[2]W. Trzebiatowski Institute of Low Temperature and Structure Research
50-950 Wroclaw, Poland

[3]Department of Physics, University of Uppsala
S-75121 Uppsala, Sweden

Magnetic susceptibility χ of uranium compounds UX_3 (X = Al, Ga, Si, Ge) is studied under pressure up to 2 kbar in the temperature range 78–300 K. A pronounced pressure effect has been revealed, and the measured volume derivatives, $d\ln\chi/d\ln V$, were found to be almost temperature-independent and equal to 2.3, 6.8, and 6.9 for USi_3, UGa_3, and UGe_3, respectively, at 78 K. In UAl_3, a noticeable temperature dependence of this derivative was obtained, ranging from $d\ln\chi/d\ln V$ = 11 at low temperatures to about 5.5 at T = 300 K. The volume dependent electronic structures of the UX_3 compounds have been calculated ab initio in the paramagnetic phase by employing a relativistic full-potential LMTO method. The calculations have brought out a predominance of itinerant uranium 5f states at the Fermi energy. The calculated field-induced magnetic moments in UX_3 and their volume derivatives are in agreement with the experimental data on χ. An origin of the observed strong temperature dependence of the magnetovolume effect in UAl_3 is also discussed.

Introduction

Actinide compounds cover a kind of intermediate region between itinerant 3*d* and localized 4*f* compounds, and these 5*f* systems have raised a number of issues that remain to be resolved, in particular, whether the 5*f* states should be treated as itinerant or localized [1,2]. Intermetallic compounds UX_3, where X is a non-transition element from the group-III or group-IV series, crystallize in the cubic $AuCu_3$-type structure, and the U–U spacing in all compounds is far above the critical Hill limit [1–3]. Therefore the direct 5*f*–5*f* interactions are presumably weak, and these compounds provide an exceptional opportunity to study the role of *f*–*spd* hybridization in magnetic properties, ranging from Pauli-

like paramagnetism (USi_3 and UGe_3) and itinerant antiferromagnetism (UGa_3) to assumed spin-fluctuation behavior (UAl_3 and USn_3) and local-moment ordering (UIn_3, UTl_3, UPb_3) [1–10]. In this connection, the main objective of the present work is to shed light on the nature of magnetism in a representative series of UX_3 compounds. For this reason the pressure effect on magnetic properties of UX_3 has been investigated both experimentally and theoretically. Specifically, the pressure derivatives of the magnetic susceptibility, χ, derived from the measurements under pressure, are of particular interest, owing to their sensitivity to the nature of magnetism. The experimental study is complemented by *ab initio* calculations of the volume-dependent band structure and field-induced magnetization of UX_3 compounds in the paramagnetic phase. These calculations allowed to elucidate some features of the electronic structure, which are presumably responsible for peculiar magnetic properties of UX_3. The calculated pressure effect on magnetization has been directly compared with the experimental data.

Experiment

The polycrystalline samples of UAl_3, UGa_3, USi_3 and UGe_3 were prepared by arc-melting of the constituent metals in an argon atmosphere and subsequent annealing under vacuum at 600°C. These samples were checked by X-ray powder diffraction and found to be single phases crystallizing in the $AuCu_3$ crystal structure. Firstly, the temperature dependences of χ over a wide temperature range (4.2 to 300 K) were measured at ambient pressure by the Faraday method with the relative errors of about 0.3%. The onset of the antiferromagnetic order was observed only for UGa_3 at T = 67 K, in agreement with previous studies [5,8,9] on the single-crystalline samples. Other compounds, UAl_3, USi_3 and UGe_3, did not show any evidence of magnetic ordering down to 4.2 K. As an illustration, the $\chi(T)$ dependence for UAl_3 is shown in Fig. 1.

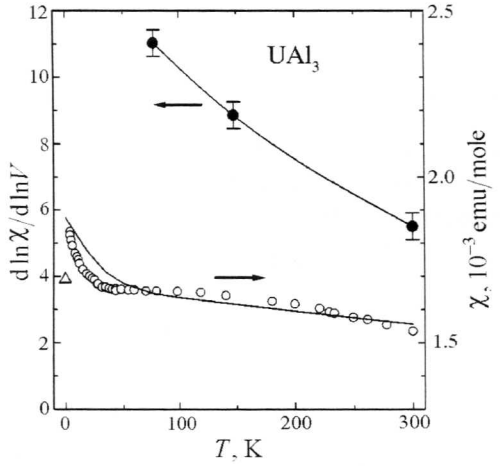

Fig. 1. The measured temperature dependences of the magnetic susceptibility χ (open circles, at ambient pressure) and the $d\ln\chi/d\ln V$ derivative (filled circles) for UAl_3. For comparison there are also presented the experimental $\chi(T)$ of Ref. [3] (solid line) and the low-temperature data on χ of Ref. [7] (open triangle)

The magnetic susceptibility was studied under helium gas pressure up to P = = 2 kbar, for the most part at temperatures of 78 and 300 K. The measurements were carried out by the Faraday method, using a pendulum magnetometer placed into the pressure cell [11]. The relative errors of our measurements did not exceed 0.05% for magnetic fields used (H = 1.7 T). The pressure dependence of the susceptibility, $\chi(P)$, appeared to be linear for all UX_3 compounds studied. In order to transform the experimentally obtained pressure derivatives, $d\ln\chi/dP$, into the volume derivatives, we made use of the experimental bulk moduli from Ref. [12]. The resulting values of $d\ln\chi/dP$ and $d\ln\chi/d\ln V$ are listed in Table 1.

Table 1

Magnetic susceptibility χ and its pressure and volume derivatives in UX_3 compounds (X = Al, Ga, Si, Ge)

System	T, K	$\chi\cdot10^3$, emu/mole		$d\ln\chi/dP$, $Mbar^{-1}$	$d\ln\chi/d\ln V$	
		experiment	theory	experiment	experiment	theory
UAl_3	78	1.66	–	–	11.0 ± 0.4	–
	–	–	–	10.2 ± 0.4	–	–
	148	1.67	–	–8.2 ± 0.4	8.9 ± 0.4	–
	300	1.53	1.55	–5.1 ± 0.4	5.5 ± 0.4	6
UGa_3	78	1.95	–	–6.8 ± 0.3	6.8 ± 0.3	–
	300	1.74	1.67	–5.4 ± 0.3	5.3 ± 0.3	6.3
USi_3	78	0.58	–	–1.8 ± 0.7	2.3 ± 0.9	–
	300	0.57	0.59	–2.0 ± 0.6	2.5 ± 0.8	3.9
UGe_3	78	1.06	–	–5.1 ± 0.7	6.9 ± 1.0	–
	300	1.12	1.19	–4.9 ± 0.6	6.6 ± 0.8	6.1

The $\chi(T)$ dependence of UGa_3 was investigated in the vicinity of the Neel temperature for different pressures. The resulting pressure derivative, $dT_N/dP = -1.1 \pm 0.2$ K/kbar, is in close agreement with the value reported in Ref. [5], $dT_N/dP = -1.4$ K/kbar, which has been derived from resistivity measurements on a single-crystalline sample of UGa_3. Extrapolation gives that the antiferromagnetic (AFM) order is expected to disappear at a critical pressure of 50 kbar. The corresponding logarithmic volume derivative of the Neel temperature, $d\ln T_N/d\ln V = 16 \pm 3$, is comparable to the corresponding value found for another itinerant antiferromagnetic uranium compound, UN ($d\ln T_N/d\ln V = 19$, Ref. [1]).

Theory

Electronic band structures of the paramagnetic UX_3 compounds (X = Al, Ga, Si, Ge, Sn) are calculated *ab initio* by employing the full-potential LMTO method [13] (FP-LMTO). The band structure of the low-temperature AFM phase of the UGa_3 compound was studied recently in detail in Ref. [9,10], and here we need to focus on the paramagnetic phase of UGa_3 (above T = 67 K), which is relevant to the present experimental investigations of χ under pressure. The von Barth-Hedin parametrization [14] was employed for the exchange-correlation potential in the framework of the local spin density approximation (LSDA). The spin-orbit coupling was included at each variational step of the self-consistent calculations. The integration over the Brillouin zone was performed using the special point sampling and with a Gaussian smearing of 10 mRy (see details in Ref. [13]). After achievement of convergency for the total energy, the densities of electronic states (DOS) $N(E)$ were obtained on a fine energy mesh, and presented here in Fig. 2,*a–e*.

The UX_3 band structures calculations were performed for a number of lattice parameters close to experimental ones. The equilibrium lattice spacings, a, and bulk moduli, B, were evaluated from the calculated total energies E as functions of volume V. The $E(V)$ dependences, obtained for UX_3, were fitted to analytical parametrizations for the equation of state, such as the Murnaghan and recently proposed universal [15] equations. As can be seen in Table 2, the evaluated theoretical lattice spacings and bulk moduli are in a reasonable agreement with experimental data [12]. The calculated equilibrium volumes appeared to be smaller than the experimental ones, which is a rather normal underestimation when LSDA is used in combination with FP-LMTO [13]. This is apparently due to the overbonding tendency of LSDA, which also provides overestimated values of B in Table 2.

Table 2

Bulk and electronic properties of UX_3*

Compound	a_{exp}, Å	a_{theor}, Å	B_{exp}, GPa	B_{theor}, GPa	$N_{theor}(E_F)$, states/Ry·cell	$N_{exp}(E_F)$, states/Ry·cell	λ
UAl_3	4.251	4.12	108	120	80	249	2.1
UGa_3	4.261	4.10	99	110	92**	300	2.25
USi_3	4.033	3.92	125	140	53	81	0.5
UGe_3	4.205	4.08	136	150	70	118	0.7
USn_3	4.612	4.47	83	110	120	992	7.3

*Experimental lattice parameters a and bulk moduli B are taken from Ref. [12]. Experimental DOS at the Fermi level, $N_{exp}(E_F)$, are obtained by Eq. (2) from the measured electronic specific heat coefficients in Ref. [3,5,9]. The corresponding many-body enhancement parameters λ are evaluated according to Eq. (3).

**DOS of the low-temperature AFM phase of UGa_3, calculated in Ref. [9].

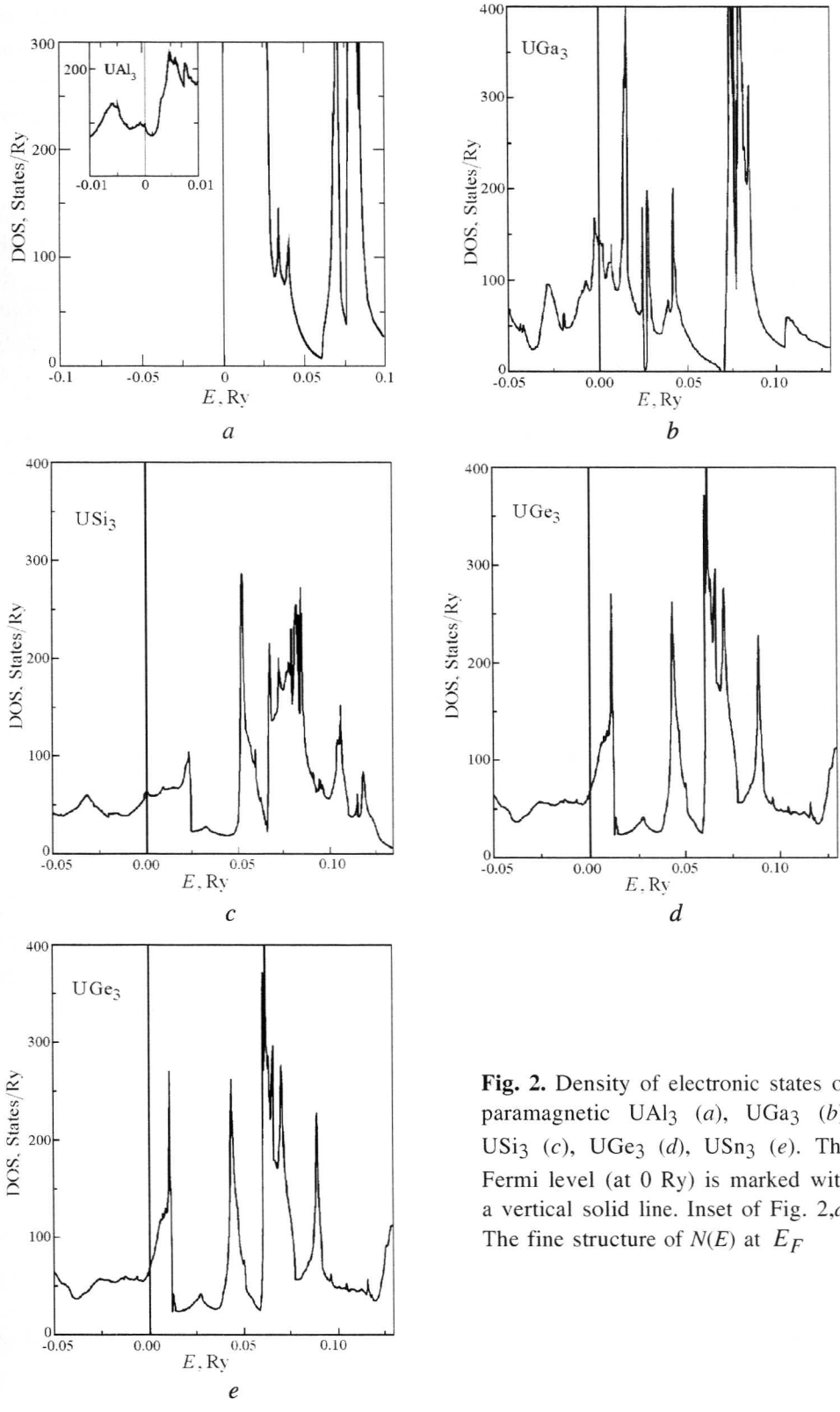

Fig. 2. Density of electronic states of paramagnetic UAl_3 (*a*), UGa_3 (*b*), USi_3 (*c*), UGe_3 (*d*), USn_3 (*e*). The Fermi level (at 0 Ry) is marked with a vertical solid line. Inset of Fig. 2,*a*: The fine structure of $N(E)$ at E_F

Magnetic properties of actinide systems can not be explained within the Stoner approach, because spin-orbit coupling in connection with spin polarization induces large orbital moments [16,17]. In case the spin-orbit energy dominates over the Zeeman spin polarization energy, the orbital magnetic moment is larger than, and anti-parallel to the spin moment [6,8,17]. Also, in uranium systems with less than a half-filled *f*-electronic shell the crucial parameter determining whether the spin and orbital moments are parallel or not, is the relation between the magnitude of the magnetic susceptibility and the spin-orbit parameter. Thus, the resulting moments are determined by the interaction between the Zeeman operator, exchange effects and spin-orbit coupling. In a general case, the magnitudes and directions of these magnetic moments can be evaluated from *ab initio* band structure calculations, where all above-mentioned interactions are taken into account on the same footing.

To analyze the observed pressure behavior of susceptibility, the external magnetic field was taken into account by means of the Zeeman operator, $H(2s + l)$, which has been incorporated in the FP-LMTO Hamiltonian for *ab initio* calculations of the field-induced spin and orbital moments, in line with Refs. [6,8]. In these spin-polarized calculations the external magnetic field was assigned to 10 T, and the spin and orbital magnetic moments were calculated as described in Ref. [16]. Also, the orbital polarization correction was included in the calculations according to Ref. [18]. By this way the corresponding magnetization can be evaluated, and the ratio between the magnetization and the field strength is the paramagnetic susceptibility. In the relevant range of magnetic fields, the calculated χ appeared to be field independent. The evaluated χ and the corresponding volume derivatives are given in Table 1.

Discussion

The main contributions to DOS of UX_3 compounds at the Fermi level E_F come from uranium 5*f*-states and *p*-states of ligand *X*, which overlap in energy. A strong hybridization between these states gives rise to narrow bands of itinerant states in the energy range about 0.2 Ry at E_F (see Fig. 2,*a–e*). The calculated DOS for UX_3 compounds at E_F are listed in Table 2 together with «experimental» values of $N_{\text{exp}}(E_F)$, which were obtained from the measured [3,5,9] electronic specific heat coefficients:

$$C/T = \gamma + \beta T^2 + \delta T^2 \ln T\,, \tag{1}$$

where γ is the temperature electronic specific heat coefficient given by

$$\gamma = 2\pi^2 k_B^2 N_{\text{exp}}(E_F)/3\,. \tag{2}$$

The $N_{\text{exp}}(E_F)$ values are apparently enhanced with respect to the theoretical DOS at E_F, $N_{\text{theor}}(E_F)$, presumably due to the many-body effects:

$$N_{\text{exp}}(E_F) = (1 + \lambda)N_{\text{theor}}(E_F)\,. \qquad (3)$$

The enhancement parameters λ, evaluated by Eq. (3), are also listed in Table 2. These parameters are usually linked to the electron-phonon interaction, $\lambda_{\text{e-ph}}$, though a spin-fluctuation (SF), or paramagnon enhancement, λ_{SF}, can contribute to the total λ as well. The second effect of spin fluctuations in the specific heat C can be represented by the third term in Eq. (1), $\delta T^2 \ln T$, which, in conjunction with the linear electronic term, appears as a low-temperature upturn in C/T versus T^2 curve [2]. This additional SF term was taken into account in the experimental specific heat studies for UX_3 [5,9] to evaluate the reliable electronic coefficient γ. It turns out that the specific heat data for UGa_3 and USn_3 are fit well to Eq. (1) even without the inclusion of the SF term. In the case of UAl_3, however, the accurate fit requires the SF term taken into account in Eq. (1) [9]. It may be suggested that the increase of λ in the series USi_3, UGe_3, UGa_3, UAl_3, USn_3 (see Table 2), most likely can be related to the SF contribution λ_{SF}, rather than to the electron-phonon enhancement $\lambda_{\text{e-ph}}$.

The calculated field-induced spin and orbital magnetic moments appeared to be almost exclusively of $5f$ character and anti-parallel in each UX_3 compound, in agreement with the Hund's third rule. Also, for these compounds the field-induced orbital moments are substantially larger than the spin moments. In general, the calculated total field-induced moments are in good agreement with the experimental [1,3,5,9] data on χ in UX_3 compounds (see Table 1).

For the UX_3 compounds the volume effect was found to be more pronounced for the orbital contribution to the field-induced magnetic moment than for the spin contribution. Since the orbital moment is of van Vleck-type, i.e. originating from the mixing of states across the energy bands [16,17], the magnitude of this moment is expected to be inversely proportional to the band width, W. Based on the present band structure calculations, the band width scales as $d\ln(1/W)/d\ln V \cong$ $\cong 4$. This value is in reasonable agreement with the volume derivatives of the calculated induced moments and the experimental magnetic susceptibilities, listed in Table 1. Therefore, the observed large magnetovolume effect in UX_3 is apparently related to the rapid quenching of the induced orbital moment with increasing width of the $5f$-band under applied pressure.

As can be seen from Table 1, the calculated volume derivatives of χ are in a fair agreement with the corresponding experimental derivatives of the magnetic susceptibility. These results indicate that the values of $d\ln\chi/d\ln V$ for UAl_3, UGa_3 and UGe_3 follow a general trend for UX_3 compounds in the dependence of the magnetic susceptibility on the lattice parameter a. As is seen in Fig. 3, the variation of the $\ln\chi$ versus $\ln a$ for these compounds is close to linear with the slope $d\ln\chi/d\ln a \cong 18$, which corresponds to $d\ln\chi/d\ln V \cong 6$. This trend

illustrates the dominant role that the interatomic spacing has on magnetic properties of UX_3 compounds. On the other hand, for USi_3 the experimental and calculated derivatives $d\ln\chi/d\ln V$ do not follow the same trend (see also Table 1). It should be noted, however, that the value of χ for USi_3 obtained in the present work ($0.57 \cdot 10^{-3}$ emu/mole) differs substantially from the results of earlier measurements ($0.66 \cdot 10^{-3}$ emu/mole [3] and $0.48 \cdot 10^{-3}$ emu/mole [4]), and thus a further experimental study of USi_3 seems necessary on well-attested samples.

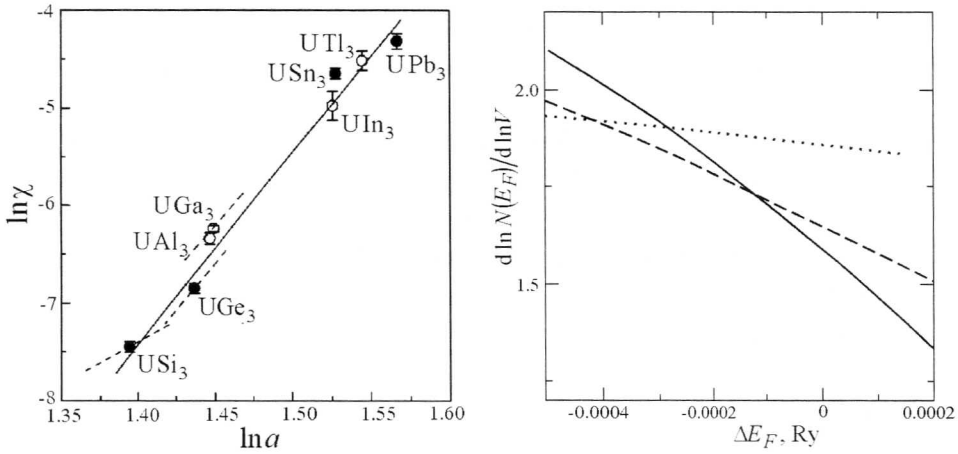

Fig. 3. Magnetic susceptibility vs lattice spacing in UX_3 compounds (on a logarithmic scale). Open circles indicate UAl_3, UGa_3, UIn_3 and UTl_3, whereas the filled circles stand for USi_3, UGe_3, USn_3 and UPb_3. The dashed lines represent the experimental $d\ln\chi/d\ln V$ derivatives for UAl_3, UGa_3, USi_3 and UGe_3. The solid line is a guide for the eye

Fig. 4. The logarithmic derivative of DOS in UAl_3 at the Fermi level with respect to the atomic volume, $d\ln N(E_F)/d\ln V$, vs variation (shift) of E_F. The solid, dashed, and dotted lines correspond to the temperatures of 78, 148, and 300 K, respectively

For UAl_3 an unusual strong temperature effect on the $d\ln\chi/d\ln V$ derivative is observed (see Table 1 and Fig. 1). In order to shed light on the origin of this effect, we studied in detail both pressure and temperature dependence of the UAl_3 band structure in the vicinity of E_F. Specifically, DOS at the Fermi level, $N(E_F)$, is closely related to the enhanced Pauli paramagnetism, χ_s, defined as:

$$\chi_s = S\chi_P = \mu_B^2 N(E_F)\left[1 - IN(E_F)\right]^{-1}. \qquad (4)$$

Here χ_P – the Pauli spin susceptibility, S – the Stoner enhancement factor, I – the effective exchange-correlation interaction between conduction electrons. Due to comparatively high Stoner enhancement in UAl_3 ($S \cong 5$, according to the

present calculations), the spin contribution χ_s is competitive with the orbital contribution, $\chi_{\text{orb}} \cong 2\chi_s$, and its volume and temperature dependence may be of some importance.

The $\mathrm{d}\ln N(E_F)/\mathrm{d}\ln V$ derivative is elaborated from the corresponding band structure calculations for a number of atomic volumes, between the theoretical and experimental ones. For finite temperatures the effect of «smearing» through the Fermi-Dirac distribution function $f(E,\mu,T)$ has been taken into account:

$$N(E_F,T) = \int N(E)\left[-\partial f(E,\mu,T)/\partial E\right]\mathrm{d}\,E\,.$$

The estimated values of $\mathrm{d}\ln N(E_F,T)/\mathrm{d}\ln V$ are presented in Fig. 4. It is clearly seen, that the temperature dependence of this derivative is strongly dependent on the initial position of the Fermi level, and the shifts ΔE_F from the *ab initio* calculated value ($E_F = 0$ in Fig. 4) are basically well within the accuracy of LSDA calculations. Therefore one can anticipate the corresponding noticeable temperature effect on $\mathrm{d}\ln \chi_s/\mathrm{d}\ln V$, provided the appropriate Stoner enhancement $S \cong 5$ is taken into account.

Basically, the strong temperature effect on the $\mathrm{d}\ln N(E_F,T)/\mathrm{d}\ln V$ derivative, and on the $N(E_F)$ itself, is related to the peculiar structure of DOS at E_F in UAl_3 (see inset in Fig. 2,*a*). Also small shifts ΔE_F in Fig. 4 can be easily expected in real samples due to minor deviations from stoichiometry. This can explain the substantially different $\chi(T)$ dependences, reported in Refs. [3,7,9] and in the present work (Fig. 1), which were obtained on different samples of UAl_3. A comprehensive analysis of experimental $\chi(T)$ curves should also take into account the volume thermal expansion and the spin fluctuations, but such analysis is obviously beyond the scope of the present study. In regard to the calculated magnetovolume effect in UAl_3, $\mathrm{d}\ln\chi/\mathrm{d}\ln V \cong 6$ in Table 1, this value was obtained by the integration over the Brillouin zone using the special point sampling with a Gaussian smearing of 10 mRy. This smearing actually means that the fine structure of DOS at E_F is averaged over a wide energy range, and the corresponding theoretical volume derivative can be ascribed to high temperatures (about 1000 K).

Conclusions

The experimental study of the magnetic susceptibility has revealed a pronounced pressure effect on χ in UAl_3, UGa_3, USi_3 and UGe_3 compounds. The observed lattice spacing dependences of χ for these systems were compared with the data available for χ in all UX_3 at ambient pressure. The comparison shows very similar volume dependence and allows to conclude that magnetic susceptibility of these UX_3 compounds is predominantly governed by the interatomic spacing variations.

The volume-dependent band structure calculations point to a strong hybridization between uranium $5f$-states and p-states of ligand in UX_3, giving a narrow band of itinerant states in the energy range about 0.2 Ry at E_F. The calculated field-induced magnetic moments of UX_3 and their volume derivatives appeared to be in a fair agreement with the experimental data on χ and $\mathrm{d}\ln\chi_s/\mathrm{d}\ln V$. This indicates the validity of the employed model of itinerant $5f$-states.

The magnetic susceptibility of the UX_3 systems is dominated by the orbital contribution χ_{orb}, which is antiparallel to the spin contribution χ_s. The volume effect is found to be more pronounced for χ_{orb}, due to the rapid quenching of the induced orbital moment with increasing width of the $5f$ band under pressure. The observed temperature dependence of the magnetovolume effect $\mathrm{d}\ln\chi/\mathrm{d}\ln V$ in UAl_3 can be related to the peculiar fine structure of DOS at the Fermi level, possible variations of E_F, and comparatively large volume effect on χ_s.

1. *J.M. Fournier, R. Troc*, in: Handbook on the Physics and Chemistry of the Actinides, North-Holland, Amsterdam (1985), v. 2.
2. *V. Sechovsky, L. Havela*, in: Ferromagnetic materials, E.P. Wohlfarth, K.H.J. Buschow (eds.), North-Holland, Amsterdam (1988). v. 4.
3. *M.H. van Maaren, H.J. van Daal, K.H.J. Buschow, C.J. Schinkel*, Solid State Commun. **14**, 145 (1974).
4. *H.R. Ott, F. Hulliger, H. Rudigier, Z. Fisk*, Phys. Rev. **B31**, 1329 (1985).
5. *D. Kaczorowski, R. Troć, D. Badurski, A. Böhm, L. Shlyk, F. Steglich*, Phys. Rev. **B48**, 16425 (1993).
6. *J. Trygg, J.M. Wills, B. Johansson, O. Eriksson*, Phys. Rev. **B50**, 9226 (1994).
7. *I. Lupsa, E. Burzo, P. Lucaci*, J. Magn. Magn. Mater. **157/158**, 696 (1996).
8. *G.E. Grechnev, A.S. Panfilov, I.V. Svechkarev, A. Delin, B. Johansson, J.M. Wills, O. Eriksson*, J. Magn. Magn. Mater. **192**, 137 (1999).
9. *A.L. Cornelius, A.J. Arko, J.L. Sarrao, J.D. Thompson, M.F. Hundley, C.H. Booth, N. Harrison, P.M. Oppeneer*, Phys. Rev. **B59**, 14473 (1999).
10. *J. Schoenes, U. Barkow, M. Broschwitz, P.M. Oppeneer, D. Kaczorowski, A. Czopnik*, Phys. Rev. **B61**, 7415 (2000).
11. *A.S. Panfilov*, Fizika i tekhnika vysokikh davlenii **2**, № 2, 61 (1992) (in Russian).
12. *T. Le Bihan, S. Heathman, S. Darracq, C. Abraham, J.M. Winand, U. Benedict*, High Temp.–High Press. **27/28**, 157 (1996).
13. *J.M. Wills, O. Eriksson*, in: Electronic structure and physical properties of solids, H. Dreysse (ed.), Springer, Berlin (2000).
14. *U. von Barth, L. Hedin*, J. Phys. **C5**, 1629 (1972).
15. *P. Vinet, J.H. Rose, J. Ferrante, J.R. Smith*, J. Phys. Cond. Matt. **1**, 1941 (1989).
16. *M.S.S. Brooks, P.J. Kelly*, Phys. Rev. Lett. **51**, 1708 (1983).
17. *M.S.S. Brooks*, Physica **B190**, 55 (1993).
18. O. Eriksson, B. Johansson, M.S.S. Brooks, Phys. Rev. **B41**, 7311 (1990).